Supplementary Information

Altering the deposition behavior and enhancing the interface stability via a gradient-potassiophilic scaffold achieve a highly efficient and dendrite-free potassium metal anode

Dongting Zhang [a, b*], Minpeng Li [c, d], Yuping Qiu [c, d], Weihai Yi [c, d], Hanyuan Che [c, d], Wenjie Shi [c, d], Ping Wang [e], Hongruo Ma [a, b], Cuiying Lu [f*], Maocheng Liu [c, d*]

[a] Gansu Natural Energy Research Institute, Gansu Academy of Sciences, Lanzhou 730046, China

[b] Key Laboratory of Solar Energy Utilization, Gansu Province, Lanzhou 730046, China

[c] State Key Laboratory of Advanced Processing and Recycling of Non-ferrous Metals, Lanzhou University of Technology, Lanzhou 730050, People's Republic of China

[d] School of Materials Science and Engineering, Lanzhou University of Technology, Lanzhou 730050, People's Republic of China

[e] School of Chemical Engineering, Jiangxi Normal University, Nanchang 330022, China

[f] Shanxi Provincial Key Laboratory of Clean Utilization of Low-Rank Coal, Yulin university, Yulin, 71900, China

* Corresponding author: zdongt1021@163.com, lucuiying126@126.com, liumc@lut.edu.cn

Experimental Section

Preparation of 3D-T host

3D-T host was prepared via simple suction filtration and etching template processes. The negatively charge single-layer Ti_3CN solution and the positively charge SiO_2 template solution was mixed and reacted to obtain Ti_3CN-SiO_2 solution. After filtering via the vacuum filtration pump, the Ti_3CN-SiO_2 film can be obtained. The SiO_2 template in as-obtained Ti_3CN-SiO_2 film can be removed via 40% HF etching method to obtain 3D-T host.

Preparation of 3D-T/TSF host

Firstly, the negatively charge single-layer Ti_3CN solution and the positively charge SiO_2 template solution was mixed and reacted to obtain Ti_3CN-SiO_2 solution (named as solution A). Secondly, the 5 mL SnF_2 (1 M) solution was added and stirred in solution A to obtain solution B. The low-potassiophilicity Ti_3CN on the separator side (T) was prepared by filtering solution A. Then the Ti_3CN-SiO_2/Ti_3CN-SiO_2-SnF_2 film was obtained by continued suction filtration of solution B. Thirdly, 3D-Ti_3CN/Ti_3CN-SnF_2 film was prepared by 40% HF etching method. After immersing and freeze-drying, the 3D-T/TSF host was obtained. The 3D-T/TSF host composed by the low-potassiophilicity Ti_3CN on the separator side (T) and a high-potassiophilicity region on the anode side employing the Ti_3CN blended with SnF_2 nanoparticles (TSF).

Material Characterizations

The crystal structures of the 3D-T and 3D-T/TSF scaffolds were characterized on a D8 Advance X-ray diffractometer (XRD, Rigaku D/MAX 2400 Japan) using Cu Kα radiation. The microstructures of the Ti_3CN, 3D-T and 3D-T/TSF were analyzed by scanning electron

microscopy (SEM, JSM-6510). The compositions of the specimens were determined using X-ray photoelectron spectroscopy (XPS, PHI 5700 ESCA). The specific surface area and porosity were obtained by Brunauer-Emmett-Teller (BET, JWBK200C). The deposition microstructures of 3D-T and 3D-T/TSF scaffolds were observed by scanning electron microscopy (SEM, JSM-6510) and the in-situ optical microscope.

Electrochemical Analysis

Electrochemical tests were performed using CR2032-type coin cells that were assembled in an Ar-filled glove box with <0.1 ppm H_2O and O_2 levels. The electrolyte was 1.0 M KFSI in DME without any additives. K//3D-T and K//3D-T/TSF half batteries were established by K metal foils as counter electrodes and 3D-T and 3D-T/TSF scaffolds as work electrodes. The voltage profiles of K nucleation on 3D-T and 3D-T/TSF scaffolds were measurement in a LAND CT2001A battery tester (LANHE, Wuhan). Symmetric cells consisted of two 3D-T and 3D-T/TSF scaffolds which deposit with 5 mAh cm^{-2} at the current density of 0.5 mA cm^{-2}. Galvanostatic cycle and rate capability tests were carried out based on symmetric batteries in a LAND CT2001A battery tester (LANHE, Wuhan). Tafel plots of symmetric batteries were tested on a CHI660D electrochemical workstation (Chenhua, Shanghai). Electrochemical impedance spectroscopy (EIS) was investigated by an AUTOLAB electrochemical workstation.

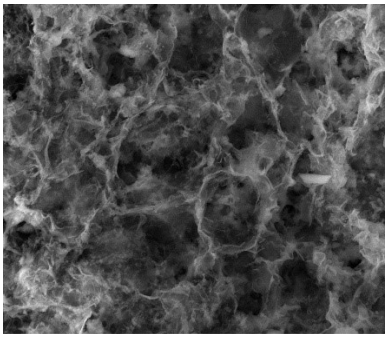

Figure S1. Top-view SEM images of 3D-T scaffold.

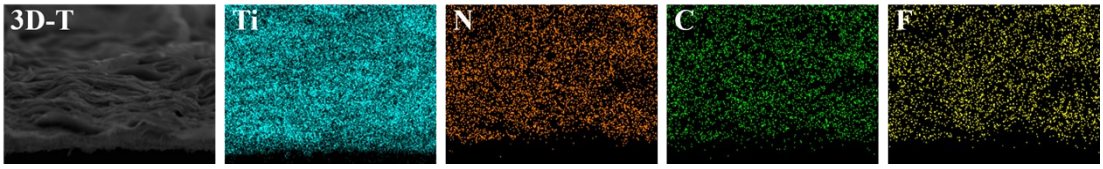

Figure S2. Cross-sectional SEM image and EDS mapping images of 3D-T host.

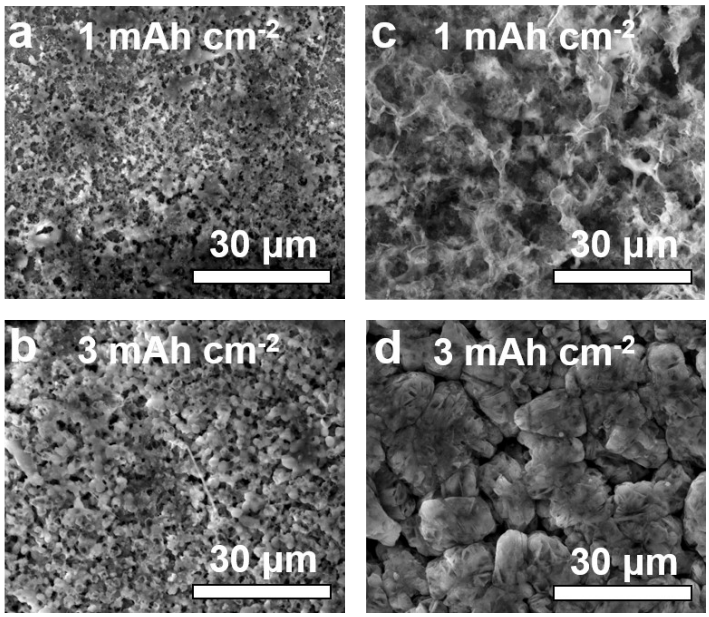

Figure S3. Top-view SEM images of 3D-T scaffold after plating a) 1 mAh cm^{-2} and b) 3 mAh cm^{-2} K metal. Top-view SEM images of 3D-T/TSF scaffold after plating c) 1 mAh cm^{-2} and d) 3 mAh cm^{-2} K metal.

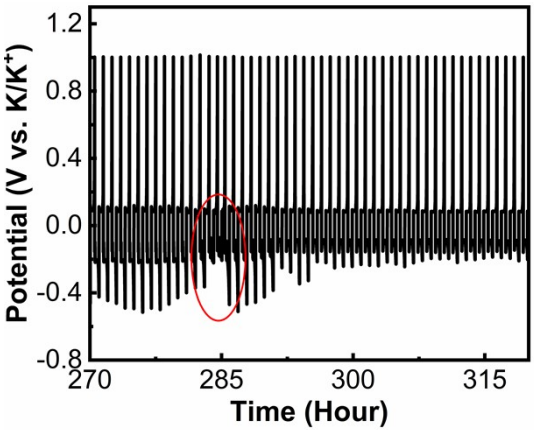

Figure S4. The high-magnification voltage-time profiles of K//3D-T half battery.

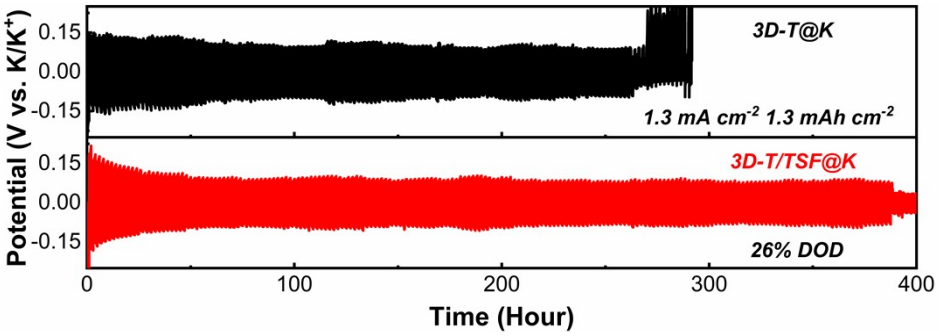

Figure S5. Cycles stability of 3D-T@K//3D-T@K and 3D-T/TSF@K//3D-T/TSF@K symmetric batteries at the current density of 1.3 mA cm^{-2} and an area capacity of 1.3 mAh cm^{-2} (26% DOD).

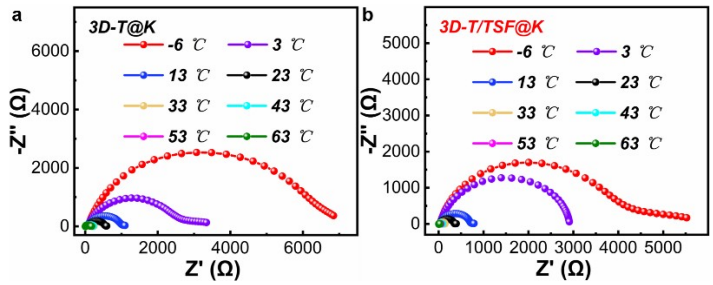

Figure S6. The EIS spectra of (a) 3D-T@K and (b) 3D-T/TSF@K symmetrical batteries at different temperature.

The R_{SEI} of 3D-T@K and 3D-T/TSF@K symmetrical batteries gradually decrease with the increased temperature. Meanwhile, 3D-T@K symmetrical battery exhibits more bigger R_{SEI} than 3D-T/TSF@K symmetrical battery.

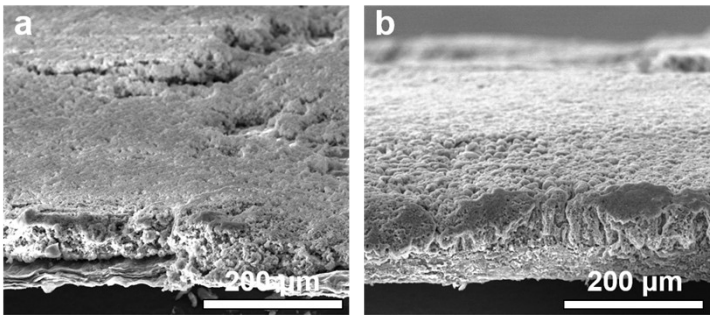

Figure S7. The Cross-sectional SEM images of a) 3D-T@K b) 3D-T/TSF@K anodes after 100th plating at 0.5 mA cm^{-2} and 0.5 mAh cm^{-2}.

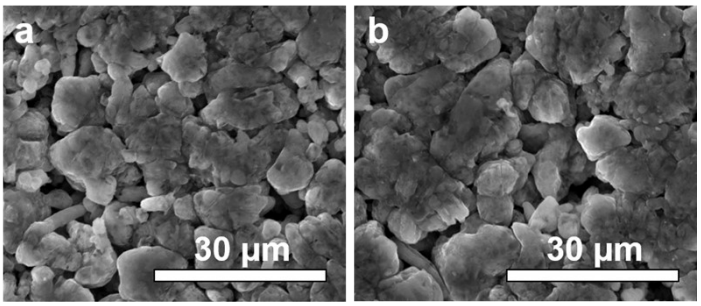

Figure S8. The top-view SEM images of 3D-T/TSF@K anode after 200 cycles at 0.5 mA cm^{-2} and 0.5 mAh cm^{-2}.

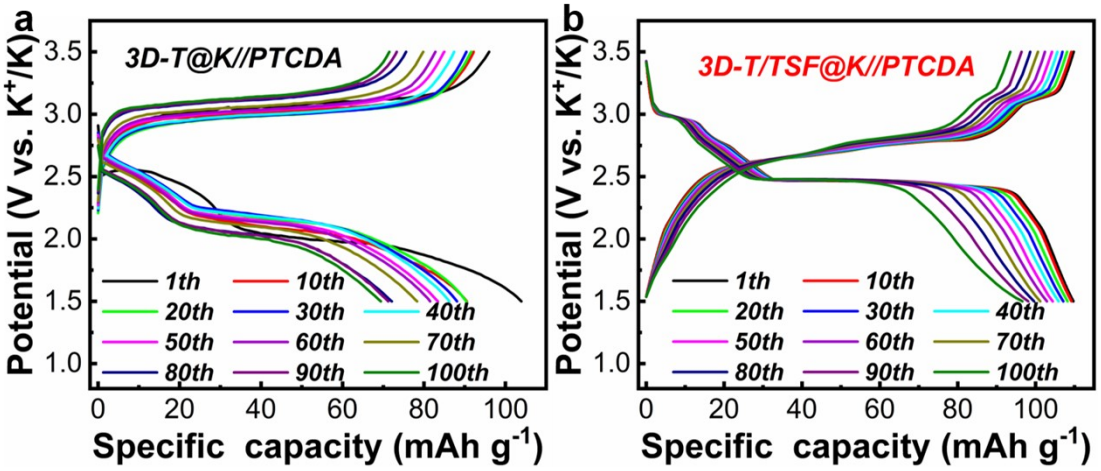

Figure S9. The charge and discharge curves after different cycles at 1C.

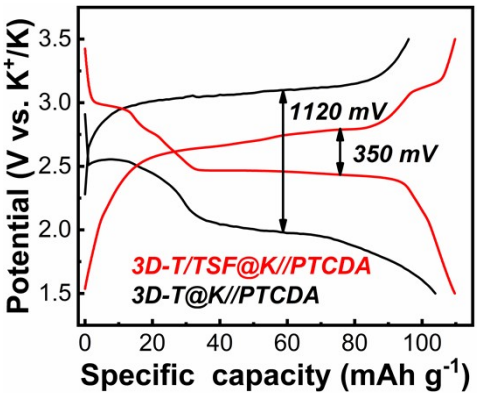

Figure S10. The initial charge and discharge curves at 1C.

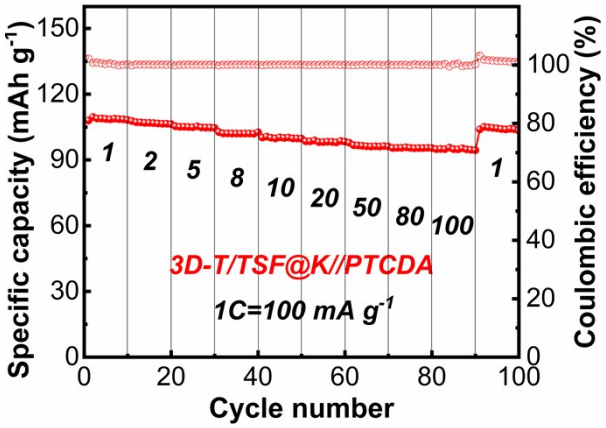

Figure 11. Rate capability of 3D-T/TSF//PTCDA full battery.